Oxidative Degradation/Mineralization of Dimethyl Phthalate (DMP) from Plastic Industrial Wastewater Using Ferrate (VI)/TiO2 under Ultraviolet Irradiation

Ping Wang (18061713169@163.com)
Nanjing Forestry University
Yi Ding
Nanjing Forestry University
Liting Zhu
Nanjing Forestry University
Yunhao Zhang
Nanjing Forestry University
Sijie Zhou
Nanjing Forestry University
Linbei Xie
Nanjing Forestry University
Ao Li
Nanjing Forestry University

Research Article

Keywords: Ferrate(VI)/TiO2/UV, Photocatalytic oxidation, Dimethyl phthalate (DMP), Response surface methodology (RSM), Industrial water treatment

Posted Date: June 23rd, 2021

DOI: https://doi.org/10.21203/rs.3.rs-441693/v1

Version of Record: A version of this preprint was published at Environmental Science and Pollution Research on October 9th, 2021. See the published version at https://doi.org/10.1007/s11356-021-16636-x.

Oxidative Degradation/Mineralization of Dimethyl Phthalate (DMP) from Plastic Industrial Wastewater Using Ferrate (VI)/TiO_2 under Ultraviolet Irradiation

Ping Wang[1] • Yi Ding[1] • Liting Zhu[1] • Yunhao Zhang[1] • Sijie Zhou[1] • Linbei Xie[1] • Ao Li[1]

✉ Ping Wang

18061713169@163.com

[1] College of Biology and the Environment, Nanjing Forestry University, Nanjing, 210037, Jiangsu, People's Republic of China

10 **Abstract**

11 A novel ferrate (VI)/titanium dioxide/ultraviolet [Fe(VI)/TiO_2/UV] system was successfully
12 established for the photocatalytic oxidation of dimethyl phthalate (DMP). This system
13 demonstrated a higher removel efficiency of DMP (95.2%) than the conventional TiO_2/UV and
14 Fe(VI) alone systems (51.8% and 23.5%, respectively), and produced obvious synergistic effects.
15 Response surface methodology (RSM), based on a three level, three independent variables
16 design, was conducted through Design Expert 8.0.6 program, and a second-order polynomial
17 model (R^2 = 0.998) was developed to quantitatively describe the photocatalysis of TiO_2
18 combined with Fe(VI) oxidation under ultraviolet irradiation. The fresh TiO_2 and photochemical
19 reacted Fe(VI)/TiO_2 were characterized by X-ray diffraction (XRD), scanning electron
20 microscope (SEM), and element dispersive spectrum (EDS), which indicated that Fe(VI) was
21 imprinted into the TiO_2, and the surface adsorbed Fe-O-(organic) materials inhibited DMP
22 degradation. This photocatalytic oxidant showed high activity and stability after nine cycles
23 without loss of its effectiveness (counting from the second cycle). The intermediates/products of
24 DMP were analyzed by gas chromatography–mass spectrometry. The proposed pathway for
25 DMP degradation involved one electron transfer of hydroxyl radical and breaking of the ester
26 bond and benzene ring. The mineralization efficiencies of DMP in actual industrial wastewater
27 and simulated water were 87.1% and 95.2%, respectively, suggesting practical field applications.
28 A ecotoxicity test (17.3% inhibition on bioluminescence) in treating actual industial wastewater
29 containing DMP implied that the proposed Fe(VI)/TiO_2/UV has a potential for industrial water
30 treatment.

31 **Keywords:** Ferrate(VI)/TiO_2/UV, Photocatalytic oxidation, Dimethyl phthalate (DMP),

Response surface methodology (RSM), Industrial water treatment

Introduction

Phthalic acid esters (PAEs) are synthetic organic compounds used as plasticizers in a broad spectrum of industrial and commercial applications. PAEs are among the wide-spread environmental contaminants worldwide (Turan et al. 2021). They are nearly ubiquitous and are detected in the air (up to μg m^{-3} level), the water (up to μg L^{-1} level), the soil and sediment (up to μg g^{-1} dw level), the food (up to mg kg^{-1} level) as well as the tissues and body fluids of humans and animals (up to μg L^{-1} level) (Martine et al. 2013; Wang et al. 2013; Zhang et al. 2015; Li et al. 2016). Dimethyl phthalate (DMP), a representative PAEs, with a hydrolysis half-life of about 3a is difficult to be degraded in nature (Staples et al. 1997).

Conventional techniques, including catalytic ozonation, gamma-radiation/H_2O_2 process (Şolpan and Mehrnia 2018), dielectric barrier discharge (Jia et al. 2018), ultraviolet (UV) photocatalysis (Jing et al. 2018; Lei et al. 2018) and biodegradation treatment (Hu et al. 2015; Zhou et al. 2017) have been extensively employed to remove DMP. Recently, biodegradation method was worldwide mostly adapted to the deep treatment of PAEs (Sarti et al. 2006). However, these compounds are difficult to be degraded in the conventional wastewater biochemical treatment systems. Traditional biodegradation is not suitable for low concentrations of DMP when considering the removal efficiency and cost. In contrast, advanced oxidation technologies have a very strong application prospect by using the extremely oxidized ·OH as an oxidant, which can completely mineralize or partially decompose these organic pollutants. Photocatalytic oxidation method utilizes a photoexcited catalyst to generate photogenerated

electrons (e_{cb}^-) and holes (h_{vb}^+)[Eq.(1)], and selectively degrades the low molecular weight organic pollutants completely without secondary pollution. Titanium dioxide (TiO_2) as a non-toxic, stable in nature, wear-resistant and inexpensive semiconductor is widely used in the field of photocatalysis (Konstantinou and Albanis 2004).

In general, the conduction band electrons (e_{cb}^-) and valence band holes (h_{vb}^+) are generated when the surface of TiO_2 is illuminated with UV light (Eq.1). Ferrate [FeO_4^{2-}, Fe(VI)], a hexavalent iron species, is a strong oxidizing agent which can be judged from the reduction potential of Eq.2 and Eq.3 in acidic and alkaline solutions, respectively (Wood 1958). Potassium ferrate (K_2FeO_4) can effectively remove organic pollutants in water, such as phenol and chlorophenol, algae and its toxins (Yuan et al. 2002; Graham et al. 2004; Sharma et al. 2010). Heterogeneous photocatalytic oxidation has been proved to be a promising water purifying method using a semiconductor material as a catalyst, to generate a highly reactive electron-hole pair to participate in and accelerate the redox reaction under ultraviolet (UV) irradiation. During the photocatalytic process, the key to improving the photocatalytic efficiency is to introduce oxidizing ions to capture electrons to reduce the chance of recombination of electrons and holes. Photoreaction of Fe(VI) may occur through three single electron steps, which results in the sequential species of Fe(V), Fe(IV) and Fe(III) (Eqs. 4 – 6). The reactivity of Fe(V) species is 10^3 – 10^5 folds higher than that of Fe(VI) (Li et al. 2005). Fe(V) ion can act as electron scavengers in the photocatalytic reactions, improving the efficiency of photoreaction (Sharma et al. 2001). The optimal combination of high-valence iron oxidation and TiO_2 photocatalysis is of great significance for developing DMP removal strategy.

$$TiO_2 + h\nu \rightarrow h_{vb}^+ + e_{cb}^- \qquad \text{(Eq.1)}$$

$E° = 3.2$ V

$FeO_4^{2-} + 8H^+ + 3e^- \rightarrow Fe^{3+} + 4H_2O$ (Eq.2)

$E° = 2.2$ V

$FeO_4^{2-} + 4H_2O + 3e- \rightarrow Fe(OH)_3 + 5OH^-$ (Eq.3)

$E° = 0.7$ V

$Fe(VI) + e_{cb}^- \rightarrow Fe(V)$ (Eq.4)

$Fe(V) + e_{cb}^- \rightarrow Fe(IV)$ (Eq.5)

$Fe(IV) + e_{cb}^- \rightarrow Fe(III)$ (Eq.6)

The demand for rapid, simple, and economical wastewater treatments to remove environmental organic pollutants has stimulated the investigation of Fe(VI)/TiO_2/UV strategy. This combination of Fe(VI) oxidation and TiO_2 photocatalysis is a promising technique that can exploit the high oxidative potential of highly reactive species [electrons (e_{cb}^-) and holes (h_{vb}^+)] to achieve either complete or partial decomposition of recalcitrant and toxic organics. Ferrate (VI) has been the most widely used metal catalyst to mediate the activation of TiO_2 using UV light (Eq.1), because it is cost-effective, low toxic, and easy to handle. In recent years, several investigations have been reported on the degradation of environmental pollutants by Fe(VI) photocatalytic combinations. Specifically, Ma et al. (2015) reported that the sulfonamides such as sulfadiazine, sulfamethoxazole and sulfadimethylpyrimidine were reduced by 89.2%, 82.0% and 83.4%, respectively, after 10 min with the treatment of Fe(VI)/TiO_2/UV. Winkelmann et al. (2008) also studied the photocatalytic degradation of cyanate (NCO^-) with Fe(VI)/UV/TiO_2/NCO^- system.

However, major challenges exist for applying homogeneous TiO_2 activation by Fe(VI)

97 under UV irradiation: the pH must be within a strict range, the amounts of Fe(VI) and TiO_2 must
98 be optimized. Ferrate (VI) is an effective oxidant and disinfectant, which promotes the
99 photocatalytic oxidation of organic pollutants. An insufficient amount of Fe(VI) provides a low
100 treatment efficiency, while excessive Fe(VI) can consume the amount of electrons, thus
101 affecting the removal of organic pollutants, as in Eqs.2 and 3. Meanwhile, to control the release
102 of soluble Fe(VI) into water solution, TiO_2, a novel supporting material, with the ability to
103 effectively immobilize soluble Fe(VI) species is expected to control the release of Fe(VI) and to
104 enhance the activation efficiency for practical environmental remediation.

105 In this study, a Fe(VI)/TiO_2/UV system was prepared to evaluate its photocatalytic and
106 oxidative properties toward the removal of DMP. Herein, TiO_2 was utilized as a photocatalyst,
107 and Fe(VI) was as an oxidant. The influence of the experimental parameters (pH, initial
108 concentrations of DMP, K_2FeO_4 and TiO_2) on DMP removal was optimized using response
109 surface methodology (RSM). The main objective of this study was to investigate the removal
110 kinetics of DMP by the Fe(VI)/TiO_2/UV system, and to assess the potential of this system for
111 the photocatalytic oxidation of DMP in industrial water treatment. The possible removal
112 mechanism of DMP was initially studied. Furthermore, the ecotoxicity of plastic industrial
113 wastewater solutions after Fe(VI)/TiO_2/UV oxidation was tested on *Vibrio fischeri*.

114 Materials and methods

115 Materials and chemicals

116 DMP (purity > 98.7%) was purchased from Aldrich Chemical Company. Sodium borate
117 ($Na_2B_4O_7 \cdot 10H_2O$) and sodium phosphate dibasic (Na_2HPO_4) which used as buffer solutions

were purchased from Nanjing Chemical Reagent Company. K_2FeO_4 (purity > 95%) and Degusa P-25 TiO_2 were obtained from Shanghai Maclean Biochemical Technology Company. All chemicals were of analytical grade and were used without further purification. The stock solution of K_2FeO_4 was prepared by dissolving 2.52 mol/L K_2FeO_4 with a pH of 9.0 and used within 10 min to minimize the self-decomposition of Fe (VI). DMP solutions were prepared by stirring 24 h at 25.0 ± 1.0°C. 0.01% HCl or 0.01% NaOH was used for pH adjustment. All the solutions were prepared with deionized water (18.0 MΩcm, Milli-Q Millipore, Waters Alliance, Milford, MA, USA).

Photocatalytic experiments

Photocatalytic experiments were conducted in a 2000 mL quartz reactor equipped with two peripheral immobilized 9 W UV lamps (PL-S 9W/10/2P, PHILIPS) at 25.0 ± 1.0°C through a thermostat circulator (THD-2015, Tianheng, China)(supporting information, Fig. S1). The emission wavelength was at 365 nm (Fig. S2). Unless otherwise stated, the experiment was started with the addition of certain amounts of Fe(VI)/TiO_2 into the aqueous solutions containing desired amounts of DMP in dark. Initial pH was adjusted by 0.01% HCl or 0.01% NaOH, and then measured by pH-meter (Mettler Toledo Five Easy Plus pH-Meter, Shanghai, China). The prepared Fe(VI)/TiO_2 – DMP solutions were kept in the dark for 30 min to achieve adsorption/desorption equilibrium. Afterwards, the photodegradation was started; water samples were withdrawn at regular intervals and analyzed immediately after filtration through 0.45 μm membrane. Finally, the photoreaction was terminated by the addition of sodium sulfate. The photochemical reacted Fe(VI)/TiO_2 was centrifuged (7000 rpm, 5 min) to be separated from the solutions and then was prepared for the following characterization analysis.

Meanwhile, the fresh TiO_2 and photochemical reacted Fe(VI)/TiO_2 were characterized by X-ray diffraction (XRD) spectra, scanning electron microscope (SEM), and element dispersive spectrum (EDS). The XRD pattern of samples' architectural feature was recorded by a Rigaku D/MAXIIIA X-ray Diffractometer. The microstructure of samples' external surface was measured with a Hitachi S-4500 SEM. The elements (C, Ti, O, and Fe) distributed on the TiO_2 surface were detected by EDS.

Analytical quantification

The degradation efficiency (η_{DMP}, %) of DMP and mineralization efficiency (η_{TOC}, %) of total organic carbon (TOC) were measured to evaluate the photo-degradability. The concentrations of DMP were analyzed by high performance liquid chromatography (Agilent 1100, USA) equipped with UV230+ UV-Vis detector and Acclaim TM C_{18} column (250 mm × 4.6 mm, 5 μm). The mobile phase was methanol: water (70:30, v/v), flow rate was 1.0 mL/min, and UV wavelength was 227 nm (Wang et al. 2012, 2015). Concentration of Fe(VI) was determined by UV-vis spectrophotometer (Shimadzu UV-2550, Tokyo, Japan) at a wavelength of 510 nm (ε_{510nm} = 1150 M^{-1} cm^{-1}). The intermediates of DMP degradation were analyzed by gas chromatography-mass spectrometry (GC-MS)(Trace ISQ, Thermo Scientific, USA) fitted with a fused capillary column (DV-1, 15 m long, 0.25 mm diam.). The initial temperature was 100°C and rose to 300°C at 10 °C/min. The injection volume was 0.5 μL. The mass spectrometer was operated at electron ionization energy of 70 eV (Wang and Fan 2014).

The wastewater was collected from Changzhou Juli Plastics Co., Ltd. The inflow and effluent of wastewater in this plant were 100 m^3 d^{-1} and 96 m^3 d^{-1}, respectively. The water parameters analyses for the wastewater were carried out before and after the treatment according

to APHA procedures (APHA 2012). Additionally, total organic carbon (TOC) was determined by a TOC analyzer (Model 1010, O.I. Analytical, NY) equipped with nondispersive infrared (NDIR) detector, with carrier gas of N_2, oxidant of 10% sodium peroxydisulfate, and TOC standard solution of anhydrous potassium biphthalate. The simulated water containing DMP 0.32 mg L^{-1} was prepared, based on the DMP concentration measured in the wastewater. All the experiments were performed in triplicate. The relative standard deviation of quantitative analysis with triple measurements was below 5%.

Optimization of multivariable by RSM

RSM was used to construct a mathematical model to quantitatively detect the interaction among TiO_2, K_2FeO_4 and pH. Three levels of pH (7.0, 9.0 and 11.0), TiO_2 (20, 40 and 60 mg L^{-1}), and K_2FeO_4 (10, 30 and 50 mg L^{-1}) were selected as independent variables and designated as χ_1, χ_2 and χ_3 respectively, as shown in Table 1. The interaction between variables and responses was found out by analyzing data using Design Expert 8.0.6 program.

Table 1 Levels of independent variables for the response surface design

Levels of independent variables for the response surface design

Independent variable	Factor level		
	–1	0	1
χ_1 (pH)	7.0	9.0	11.0
χ_2 (TiO_2 dosage, mg L^{-1})	20	40	60
χ_3 (K_2FeO_4 dosage, mg L^{-1})	10	30	50

Ecotoxicity assessment

The ecotoxicity assessment of wastewater was conducted with the standard Microtox® toxicity test system (Microbics Crop., Carlsbad, CA, USA). 2.0 mL of sample was taken directly from the water treatment system and supplied NaCl to reach 2% final concentration. The pH of samples was adjusted to 7.0 ± 0.1 using 0.01% HCl or 0.01% NaOH. The bioluminescence

intensity of *Vibrio fischeri* exposed to the sample solutions for 15 min was measured using a Dxy2 biological toxicity analyzer (Institute of Soil Science, Academia Sinica, Nanjing, China). The inhibition of bioluminescence was used to assess the acute ecotoxicity of DMP solutions prior to and after water treatment. The results were compared to an aqueous control.

Results and discussion

Optimization of DMP degradation conditions by RSM

RSM is a multivariate statistical technique for determining the optimal conditions for multivariable systems and can predict the combined effects of experimental variables. It is less laborious and time-consuming than other approaches that applied to optimize a complex process. Based on the results of a single-factors test (Fig. S3), a three-factor, three-level Box-Behnken design was utilized for the mathematical modeling of DMP degradation efficiency as a function of pH, TiO_2 dosage and K_2FeO_4 dosage. The experimental design along with the maximum observed and predicted degradation efficiency was listed in Table 2. The degradation behavior of Fe(VI)/TiO_2/UV system was fitted to the following second-order polynomial equation using multiple regression analysis.

$$\eta_{DMP}\ (\%) = +90.59 - 1.76\chi_1 + 15.50\chi_2 + 1.86\chi_3 + 0.17\chi_1\chi_2 + 0.44\chi_1\chi_3 - 0.69\chi_2\chi_3 - 14.24\chi_1^2 - 14.41\chi_2^2 - 23.22\chi_3^2 \quad \text{(Eq. 7)}$$

The data calculated by ANOVA for Eq. 7 was listed in Table 3. The F-value was the ratio between mean square of factors in different groups and mean square of factors in same group. The F-value and P-value of the model were 338.83 and < 0.0001, respectively, indicating that the regression model was extremely significant. The coefficients for the pH (χ_1), TiO_2 dosage (χ_2)

and K_2FeO_4 dosage (χ_3) were significant ($P < 0.05$). And a coefficient R^2 value of 0.998 showed that Eq. 7 was highly reliable, the model also revealed statistically insignificant lack of fit ($P = 0.8227$), which indicated that the model was adequate for prediction within the ranges of variables.

Table 2 Response surface Box-Behnken design and the experimental and predicted removal of DMP

Run	Factor			η_{DMP} (%)	
	χ_1/pH	χ_2/TiO_2 dosage (mg L^{-1})	χ_3/K_2FeO_4 dosage (mg L^{-1})	Experimental	Predicted
1	7.0	40	10	53.93	53.48
2	9.0	40	30	89.25	90.59
3	9.0	40	30	89.24	90.59
4	9.0	60	10	67.14	67.30
5	7.0	60	30	78.74	79.04
6	11.0	40	50	53.22	53.67
7	7.0	40	50	56.91	56.30
8	9.0	40	30	93.48	90.59
9	11.0	60	30	76.62	75.86
10	9.0	20	50	40.16	40.00
11	9.0	60	50	69.32	69.63
12	9.0	20	10	35.22	34.91
13	11.0	40	10	48.46	49.07
14	11.0	20	30	44.81	44.51
15	7.0	20	30	47.61	48.37
16	9.0	40	30	90.51	90.59
17	9.0	40	30	90.49	90.59

Table 3 ANOVA for response surface quadratic model

	Sum of squares	Degree of freedom	Mean square	F-value	P-value
Mode	16410.06	9	712.23	338.83	< 0.0001
χ_1	24.78	1	24.78	11.79	0.0109
χ_2	1922.62	1	1922.62	914.65	<0.0001
χ_3	27.60	1	27.60	13.13	0.0085
$\chi_1\chi_2$	0.12	1	0.12	0.055	0.8213
$\chi_1\chi_3$	0.79	1	0.79	0.38	0.5587
$\chi_2\chi_3$	1.90	1	1.90	0.91	0.3729
χ_1^2	853.74	1	853.74	406.15	<0.0001
χ_2^2	874.25	1	874.25	415.91	<0.0001
χ_3^2	2271.06	1	2271.06	1080.41	<0.0001
Residual	14.71	7	2.10		
Lack of fit	2.73	3	0.91	0.30	0.8227
Pure error	11.99	4	3.00		
Total	6424.77	16			

Note: R^2 = 99.77%; R^2 (adj) = 99.74%.

Response surfaces were plotted by Design-Expert 8.0.6 software to investigate the effects of the three independent variables and their interactions on DMP degradation. As shown in Fig. 1(a), the interaction between pH and TiO_2 dosage was not significant, which was in agreement with the results of the variance. The degradation efficiency of DMP increased with TiO_2 dosage in the pH range of 7.0 – 11.0. Figure 1(a) and (b) presented that pH played an important role in the photocatalytic process because pH had a great influence on the stability of K_2FeO_4. The relationship between pH and K_2FeO_4 dosage was significant, as shown in Fig. 1(b). When the pH was between 7.0 and 11.0, K_2FeO_4 dosage was between 10.0 mg L^{-1} and 50.0 mg L^{-1}, the degradation efficiency of DMP increased with the K_2FeO_4 dosage increasing from 10.0 mg L^{-1} to 30.0 mg L^{-1} and then it decreased while K_2FeO_4 dosage increased further. The degradation efficiency increased with the increase of pH until around 9 and then it decreased at pH > 9.0. The maximum degradation efficiency of DMP was 93.48% at pH 9.0.

As shown in Fig. 1(c), the combined effect of TiO_2 dosage and K_2FeO_4 dosage was highly significant. The degradation efficiency increased firstly and then decreased with the increase of K_2FeO_4 dosage while the dosage of TiO_2 was unchanged. When the dosage of K_2FeO_4 was between 10.0 mg L^{-1} and 50.0 mg L^{-1}, the degradation efficiency of DMP increased with the increase of TiO_2 dosage. Results indicated that the maximum degradation efficiency was observed when the K_2FeO_4 dosage was 30.0 mg L^{-1}.

As shown in Table 4, the predicted optimal conditions based on the RSM were initial TiO_2 concentration of 50.73 mg L^{-1}, pH 8.89, and initial K_2FeO_4 concentration of 30.64 mg L^{-1}. To verify the accuracy and reliability of the prediction model, three parallel verification tests were performed under the optimal conditions. The degradation efficiency of DMP was 91.36 ± 2.12%. The experimental value closely agreed with the result obtained from RSM, which validated the findings of response surface optimization.

Table 4 Optimum values for the DMP degradation

Variable	Optimum value (χ_i)
Initial pH of DMP solution	8.89
Initial TiO_2 concentration, mg L^{-1}	50.73
Initial K_2FeO_4 concentration, mg L^{-1}	30.64
η_{DMP}, %	90.59 (predicted) 91.36 ± 2.12[a] (experimental)

[a] Mean ± standard deviation (n = 3)

An optimal condition could be therefore obtained as 50.73 mg L^{-1} TiO_2, 30.64 mg L^{-1} K_2FeO_4 and pH 8.89.

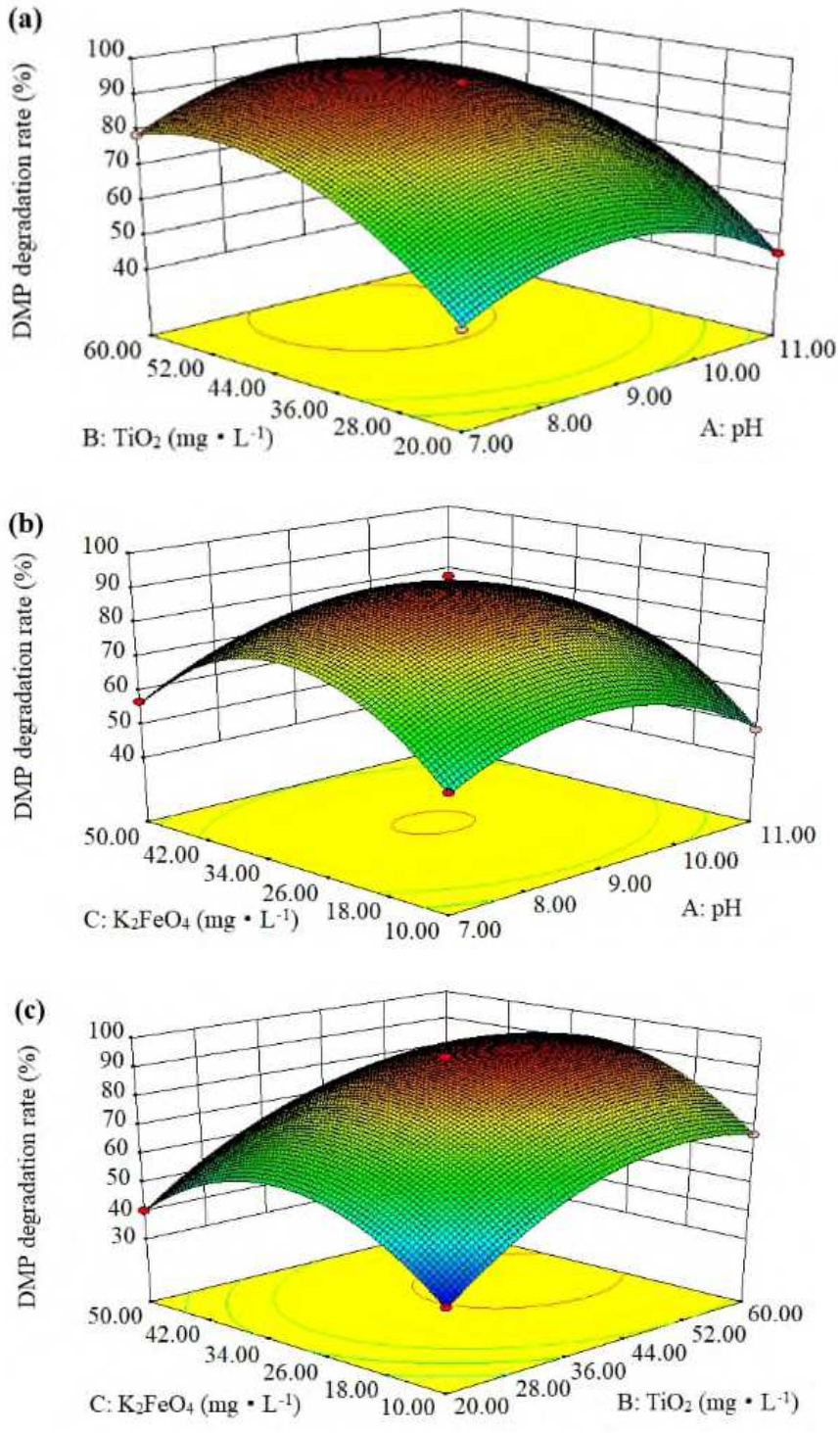

Fig. 1 3-D response surface plots for DMP degradation efficiency (%) as a function of: (a) initial pH and TiO_2 dosage at initial K_2FeO_4 concentration of 30.0 mg L^{-1}; (b) initial pH and K_2FeO_4 dosage at initial TiO_2 concentration of 50.0 mg L^{-1}; (c) TiO_2 dosage and K_2FeO_4 dosage at initial pH 9.0.

Performance of the Fe(VI)/TiO_2

Stability of ferrate(VI)

The initial concentration of K_2FeO_4 solution was 30.0 mg L^{-1}, the variation of the stability (self-decomposition) of Fe(VI) with time t (min) were observed at pH values of 7.0, 8.0, 9.0 and 10.0 in the absence of catalyst TiO_2 and UV light. The Fe(VI) concentration was determined by UV-vis Spectroscopy every 1 min. Figure 2(a) showed that there was an insignificant decrease in the amount of Fe(VI) at pH 9.0 or 10.0. The decomposition of Fe(VI) could be described with the pseudo-first-order kinetic model $\ln([Fe]_t/[Fe]_0) = -kt$ (Eq. 8). Herein, $[Fe]_0$, $[Fe]_t$ and k stand for the initial concentration (mg L^{-1}), the concentration of K_2FeO_4 (mg L^{-1}) at time t (min), and the pseudo-first-order rate constant (min^{-1}), respectively. The R^2 values for all pH values were over 0.99 (supporting information, Table S1). As illustrated in Fig. 2(b), the decomposition kinetic constant at pH 9.0 was calculated as 0.00319 min^{-1}, which was about 84.9-, 25.0-, and 2.1- fold higher than that at pH 7.0, 8.0, and 10.0, respectively. The stability of Fe(VI) was highly pH dependent. Fe(VI) was extremely unstable when pH value was under 9.0 and there was a maximum stability at pH range of 9.0 – 10.0.

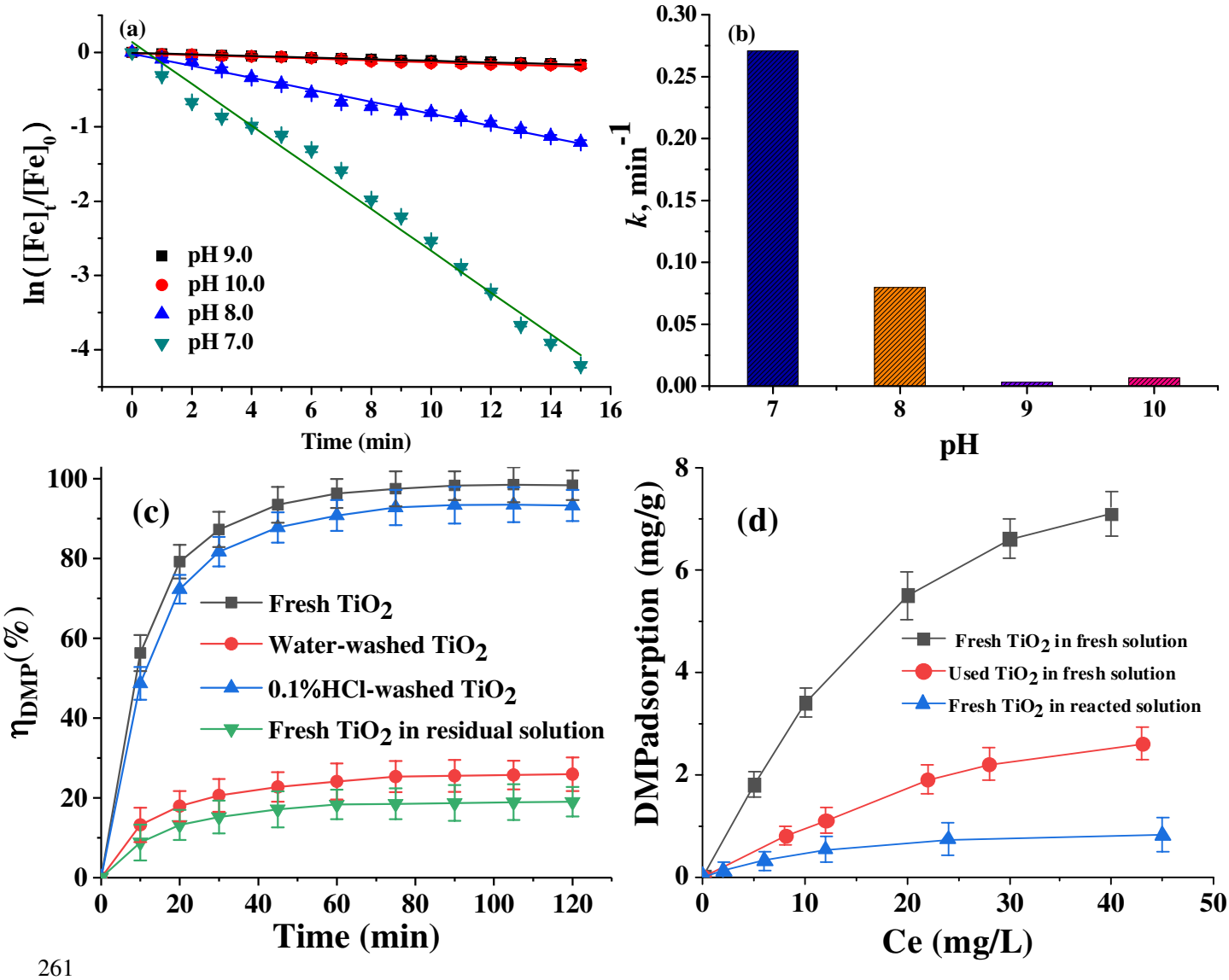

Fig. 2. (a) Decomposition of Fe(VI) in the aqueous solution ($[K_2FeO_4]_0$ = 30.0 mg L^{-1}) as a function of time, (b) their pseudo-first-order rate constants (min^{-1}) at pH 7.0, 8.0, 9.0, and 10.0, respectively. (c) Effects of different TiO_2 on the degradation efficiency of DMP, and (d) changes of DMP adsorption by different TiO_2 in fresh or reacted DMP solutions under equilibrium conditions. *Ce* (mg L^{-1}) is the concentration of DMP under equilibrium conditions. Bars represent standard deviations of three replicated measurements.

Deactivation of the TiO_2

The TiO_2 used in DMP removal was extracted by suction filtration, and then dried under vacuum. Four experimental conditions were employed with the same dose of TiO_2 (50.0 mg L^{-1}) in the presence of Fe(VI): (1) Degradation of DMP solution with fresh TiO_2; (2) Degradation of DMP solution with water-washed TiO_2; (3) Degradation of DMP solution with 1% HCl-washed

TiO_2; (4) After the solution was reacted for 120 min, degradation of residual DMP solution with fresh TiO_2. As shown in Fig. 2(c), the degradation of residual DMP solution with fresh TiO_2 and the degradation of DMP solution with water washed TiO_2 achieved low efficiency in degrading 18.3 and 24.2% respectively. However, the degradation of DMP by 1%HCl-washed TiO_2 was more than 90% within 120 min, which was similar to that of fresh TiO_2. These results disclosed that the degradation reaction by DMP might form a Fe-O-(organic) complex on the surface of the catalyst and in bulk solution, thereby inhibiting DMP degradation, and the deactivated TiO_2 catalyst could be reactivated by washing with 1% HCl solution.

Adsorption of the TiO_2

The photocatalytic degradation of DMP in aqueous solution mainly occurred on the surface of TiO_2 catalyst, and the adsorption rate of DMP on the surface of TiO_2 played a key role in the Fe(VI)/TiO_2/UV system (EL-Mekkawi et al. 2020). A number of adsorption tests were carried out in the darkness at pH 9.0 for 48 hours to determine the adsorption equilibrium. The amount of TiO_2 added in each test was 0.5 g L^{-1}. The adsorption isotherm test was carried out under the three conditions: (1) adsorption with fresh TiO_2 in fresh DMP solution; (2) adsorption with used TiO_2 in fresh DMP solution; (3) adsorption with fresh TiO_2 in reacted DMP solution. The adsorption of DMP was described with Langmuir model.

$$\frac{1}{Qe} = \frac{1}{B_L Qm} \cdot \frac{1}{Ce} + \frac{1}{Qm} \quad \text{(Eq. 9)}$$

where Q_m (mg g^{-1}) is the maximum adsorption amount of DMP adsorbed by TiO_2, Ce (mg L^{-1}) is the concentration of DMP under equilibrium conditions, Qe (mg g^{-1}) is the amount of DMP adsorbed by TiO_2 under adsorption equilibrium, and B_L is the Langmuir adsorption constant of DMP on TiO_2 surface without UV light.

As represented in Fig. 2(d), the fresh TiO_2 in the fresh DMP solution exhibited the maximum DMP adsorption, while the used TiO_2 in the fresh DMP solution and the fresh TiO_2 in the reacted DMP solution showed much lower adsorption (Priyanka et al. 2019). These results indicated that the formation of Fe-O-(organic) complexes on the surface of TiO_2 catalyst or in the bulk solution inhibits the adsorption of DMP on the surface of TiO_2.

DMP degraded very slowly in dark in the presence of Fe(VI)/TiO_2. The results depicted in Fig. S4 could be described with Langmuir – Hinshelwood model, which was expressed as follows (Eq. 10):

$$\frac{1}{k_{app}} = \frac{1}{kK_p} + \frac{C_0}{k} \quad \text{(Eq. 10)}$$

where k_{app} is the first-order rate constant (min^{-1}), k is the intrinsic reaction rate constant (mg L^{-1} min^{-1}), and K_p is the light adsorption equilibrium constant (L mg^{-1}). Figure S4(a) (pH 9.0, TiO_2 dosage 0.5 g L^{-1}) elucidated that C_0 and $1/k_{app}$ in TiO_2-Fe(IV)-UV system had a good linear relationship (R^2 = 0.960), and the slope of the line k was 0.464 mg L^{-1} min^{-1}, K_p was 0.155 L mg^{-1} calculated by the intercept. As seen in Fig. S4(b) (pH 9.0, $[TiO_2]_0$ = 0.5 g L^{-1}, $[K_2FeO_4]_0$ = 30.0 mg L^{-1}), $1/Q_e$ and $1/C_e$ has a good linear relationship (R^2 = 0.996), and B_L can be caculated from intercept and slope of the line. B_L (0.0238 L mg^{-1}) far smaller than K_p (0.155 L mg^{-1}), demonstrated that TiO_2 surface adsorption was obviously enhanced in the presence of Fe(VI) under UV irradiation.

Comparative studies of DMP degradation

To assess the extent to which mechanism contributes to the efficacy of DMP degradation, the removal rates of the six processes *i.e.*, Fe(VI) alone in dark, Fe(VI)/UV, TiO_2 alone in dark, TiO_2/UV, Fe(VI)/TiO_2 in dark and Fe(VI)/TiO_2/UV, were evaluated under the optimal operating

conditions. As shown in Fig. 3(a), the Fe(VI) or TiO_2 alone in dark had no significant effect on DMP degradation (23.4% and 20.1%, respectively), indicating that the specific organic matrix of Fe(VI) oxidation and TiO_2 catalysis had a clear selectivity. The degradation efficiency of DMP in TiO_2/UV treatment was only 51.8% within 120 min. In stark contrast, the degradation efficiency of DMP by the Fe(VI)/TiO_2/UV system reached approximately 95.2% after 120 min. As seen from Fig. 3(b), the pseudo-first order kinetic $\ln([DMP]_t/[DMP]_0) = -k_{obs}\int[Fe(VI)]dt$ could be applied for the DMP degradation in the Fe(VI)/TiO_2/UV system with a calculated k_{obs} of 2.53×10^{-2} min^{-1}. This value was about 11- and 4- fold higher than that obtained in the Fe(VI) alone in dark (2.23×10^{-3} min^{-1}), and TiO_2/UV (6.08×10^{-3} min^{-1}) systems, respectively. Comparative analysis of Fig. 3(a) – (c) demonstrated a distinct synergistic effect achieved in the combined Fe(VI)/TiO_2/UV system. Since Fe(VI) has higher oxidizing power than other electron acceptors, such as permanganate or peroxide, and may be reduced to Fe(V) with high activity. Therefore, Fe(VI) can act as an electron scavenger to enhance photo-oxidation and organic oxidation. Meanwhile, the electron scavenging of the catalyst by Fe(VI) reduction greatly reduces the recombination of the conduction band electron (e^-) and the valence band hole (h^+) in photocatalytic systems, thereby improving the quantum efficiency in the photocatalytic reaction of TiO_2 and then enhancing photocatalytic degradation of the target compound, DMP (Wong and Chu 2003).

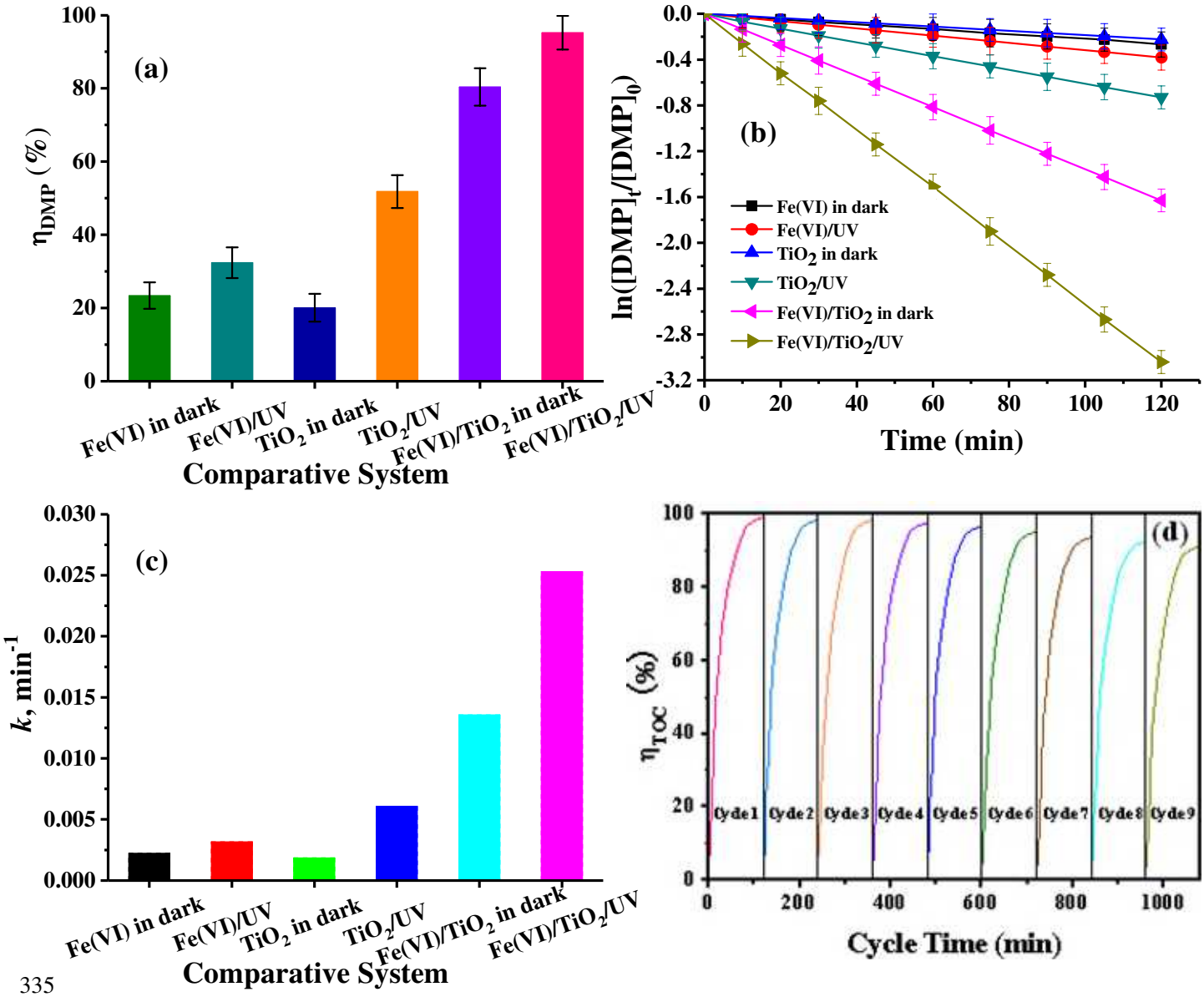

Fig. 3. Comparative studies of (a),(b) the DMP degradation, (c) pseudo-first rate constant, k, under the six processes {Fe(VI) alone in dark, Fe(VI)/UV, TiO_2 alone in dark, TiO_2/UV, Fe(VI)/TiO_2 in dark and Fe(VI)/TiO_2/UV)} under the operational condition (pH 9.0, $[DMP]_0$ = 5.0 mg L^{-1}, $[K_2FeO_4]_0$ = 30.0 mg L^{-1}, $[TiO_2]$ = 50.0 mg L^{-1}, temperature 25.0 ± 1.0°C and reaction time: 120 min), and (d) recycling performance of Fe(VI)/TiO_2/UV system. Error bars represent SD from n = 3 replicates.

Recyclability of the Fe(IV)/TiO_2

The lifetime and reusability of the catalyst are important issues for its continuous treatment of wastewater. Cycling experiments were carried out to examine the stability and reusability of Fe(VI)/TiO_2 photocatalyst *via* the degradation of DMP over nine cycles. After complete

346 degradation of each cycle, the catalyst was centrifugated from the simulated water, and carefully
347 washed with deionized water and 0.1% HCl to remove contaminants on the catalyst surface.
348 Then, the solid catalyst was dried under vacuum and reused for the next run. Figure 3d
349 displayed the results of DMP degradation for nine cycling runs. In the light of cycling
350 experimental results, η_{TOC} was 99.1% in the first run and decreased to 91.3% in the ninth cycle.
351 It could be acquired that the catalyst was stable and reusable for nine runs with a high recycling
352 performance. The reduction in photocatalytic oxidation efficiency from 99.1% to 91.3% was
353 acceptable because of DMP loss through separation and recovery and pore clogging of the
354 catalysts by DMP and its by-products. These effects reduced the specific surface area of the
355 catalysts and surface catalytic activity. Moreover, the SEM and XRD analyses of the catalyst
356 were verified before and after application to ascertain the durability of catalysts, as shown in Fig.
357 4(a)–(c). The obtained results also revealed that the catalysts were not corroded under UV
358 irradiation and maintained durable after nine cycles of DMP degradation. This was consistent
359 with the results of SEM and XRD.

360 **Characterization of the Fe(VI)/TiO_2**

361 The crystal structures of fresh and photochemical reacted Fe(VI)/TiO_2 catalysts were
362 characterized by XRD, as seen in Fig. 4(c). The peaks of Fe(VI)/TiO_2 were observed at 25.32°,
363 27.34°, 37.03°, 37.76°, 38.61°, 48.06°, 53.84°, 55.08° and 62.68°, respectively, which
364 represented Fe(VI)/TiO_2 catalyst containing anatase Mine and rutile. The mixed-phase of
365 anatase and rutile in the Degussa P25 TiO_2 had shown better photocatalytical performance than
366 pure-phase materials (Linsebigler et al. 1995; Maness et al. 1999). These XRD patterns
367 confirmed that no significant change was observed in the crystal structure of the Fe(VI)/TiO_2

368 catalyst after photocatalysis, though some dark yellow deposits were observed on the
369 photochemical reacted Fe(VI)/TiO_2 catalyst. These deposits may be $Fe(OH)_3$ or Fe-O-(organic)
370 complexes, which require further investigation. Also, SEM was used to investigate the
371 morphology of the catalyst surface. The fresh Fe(VI)/TiO_2 was round and uniform particles with
372 diameter of 25 nm, the surface structures showed a slight agglomeration, as shown in Fig. 6(a).
373 Compared Fig. 4(a) with Fig. 4(b), the morphology and particle size of fresh Fe(VI)/TiO_2 and
374 photochemical reacted TiO_2 are almost unchanged, which is consistent with XRD results. EDS
375 analysis confirmed the presence of Fe on the catalyst surface, see Fig. 4(d), the Fe content was
376 relatively small, which was consistent with the results of that the degradation reaction by DMP
377 may form a Fe-O-(organic) complex on the surface of the catalyst in bulk solution which
378 inhibited the degradation of DMP.

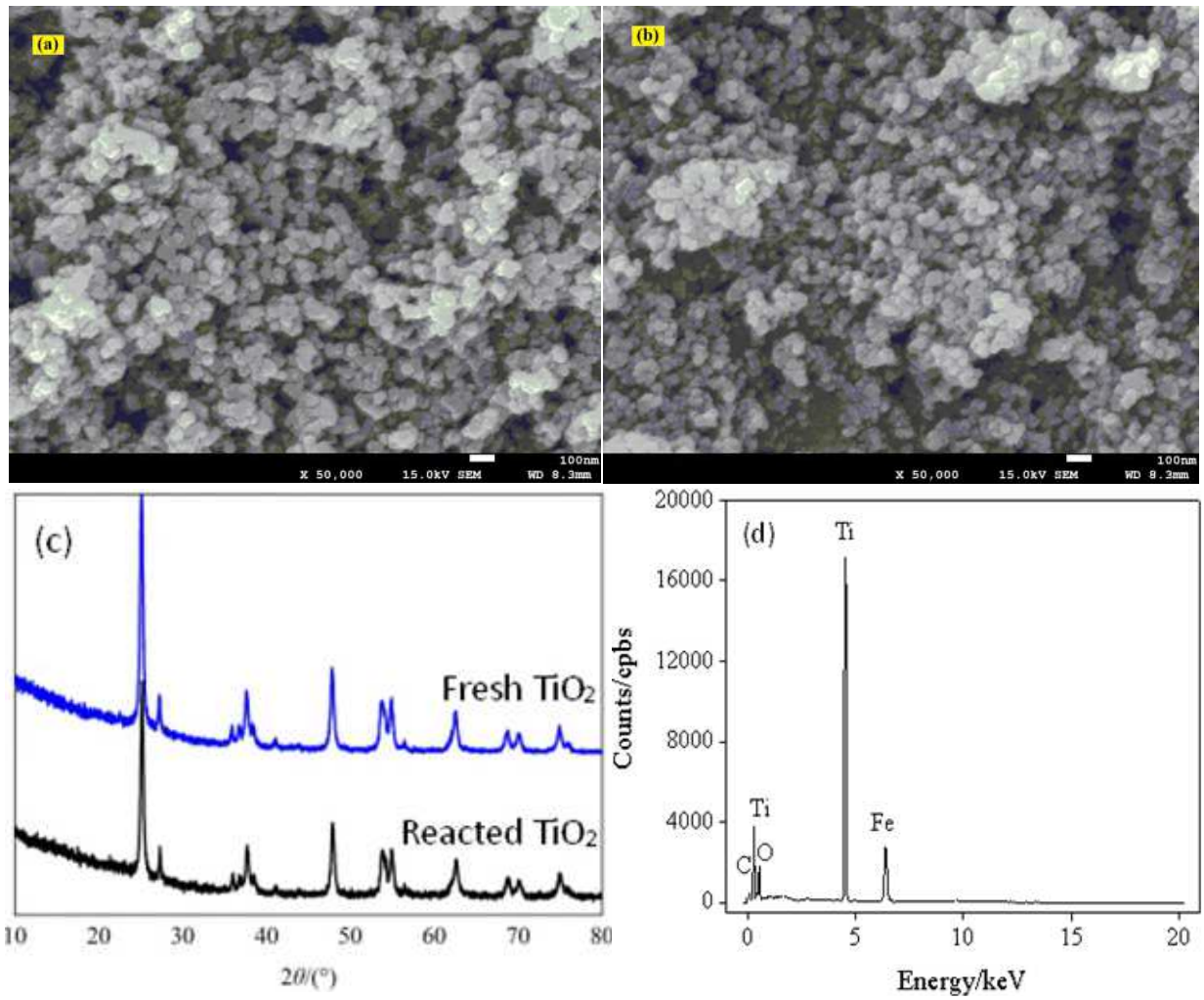

Fig. 4 SEM images of the Fresh Fe(VI)/TiO_2 (a) and photochemical Reacted Fe(VI)/TiO_2 (b). XRD pattern of the fresh Fe(VI)/TiO_2 and photochemical reacted Fe(VI)/TiO_2 (c), and EDS pattern of the photochemical reacted Fe(VI)/TiO_2 (d).

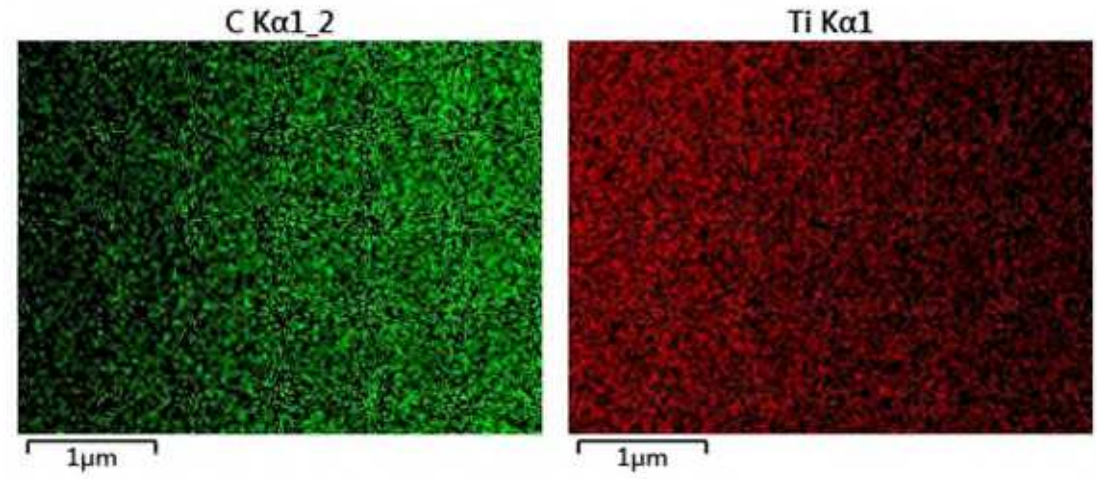

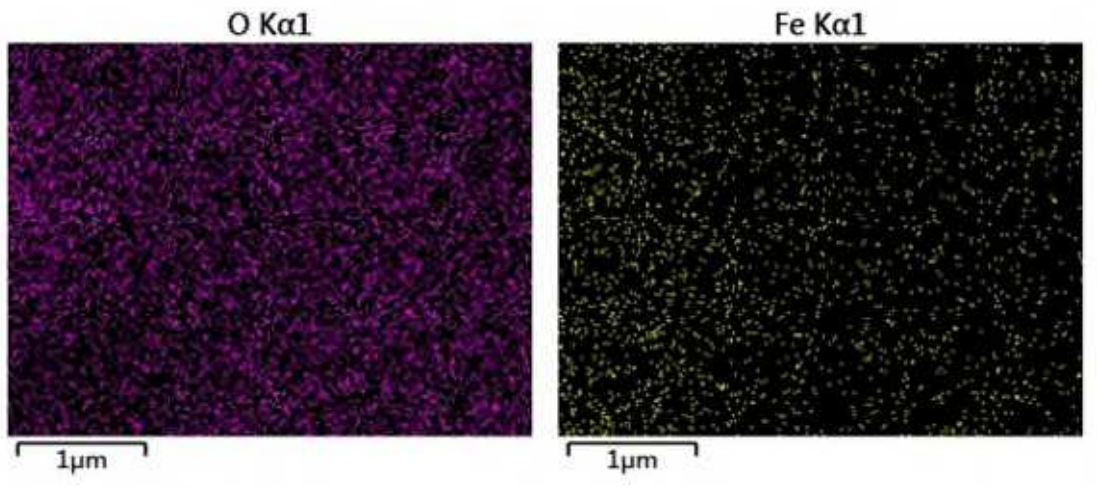

Fig. 5 EDS images of C, Ti, O and Fe attached on the surface of the photochemical reacted Fe(VI)/TiO_2

Figure 5 is the EDS images of C, Ti, O and Fe attached on the surface of the photochemical reacted Fe(VI)/TiO_2, the element Fe on the surface of Fe(VI)/TiO_2 increased obviously. Simultaneously, the high content of Ti, and the relatively low content of O were observed on the surface. This was consistent with the results that the sediments attached on the surface of the photochemical reacted Fe(VI)/TiO_2 may be Fe-O- (organic) complexes.

Degradation pathway

The intermediates of DMP degraded by Fe(VI)/TiO_2/UV system were analyzed by GC-MS (Fig. 6). Based on the identified intermediates, a degradation pathway of DMP by Fe(VI)/TiO_2/UV system was proposed as shown in Fig. 7. The main intermediate for DMP degradation was phthalic acid (PA), which was produced by electron transfer and the reactions with hydroxyl radicals. When the Fe(V) lost electrons during the process, the model compound ① could form organic cations ② and ③, respectively. The organic cation ② formed an organic substance ④ by adding a hydroxyl radical, and the organic cation ③ formed an organic substance ⑤ by adding two hydroxyl radicals. When the organic substance ④ lost a methoxy group, the observed product ⑥ (monomethyl phthalate, MMP) was formed. Product

⑥ undergone further electron loss after Fe(V) oxidation to form organic cation ⑦, organic cation ⑦ was added to a hydroxyl group, and then a methoxy group was lost to form the observed final product ⑧ (phthalic acid, PA). Alternatively, when the substance ⑤ lost two methoxy groups, it formed the final product ⑧ (phthalic acid, PA). Finally, under the action of ultraviolet light and ·OH, DMP and its benzene ring intermediates were further oxidized, and then the benzene ring would be opened to generate small molecule organic acids, and further mineralized into CO_2 and H_2O.

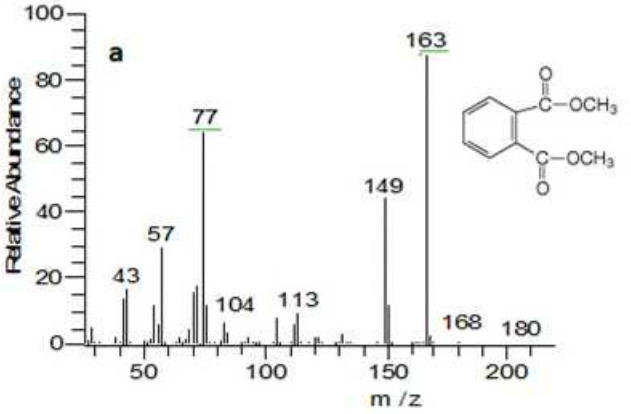

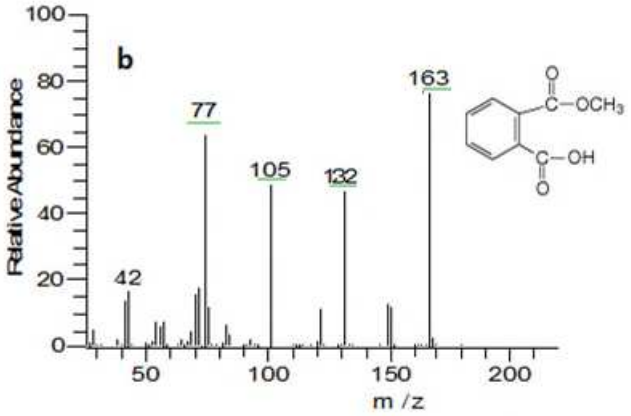

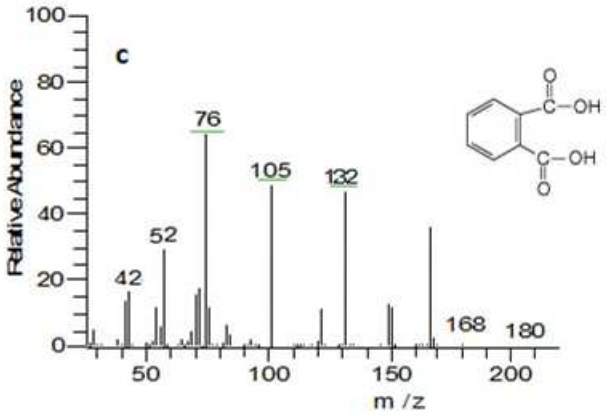

411

412 **Fig. 6** GC-MS spectra of the DMP intermediates（a：DMP；b：MMP；c：PA）degraded by
413 Fe(VI)/TiO_2/UV system.

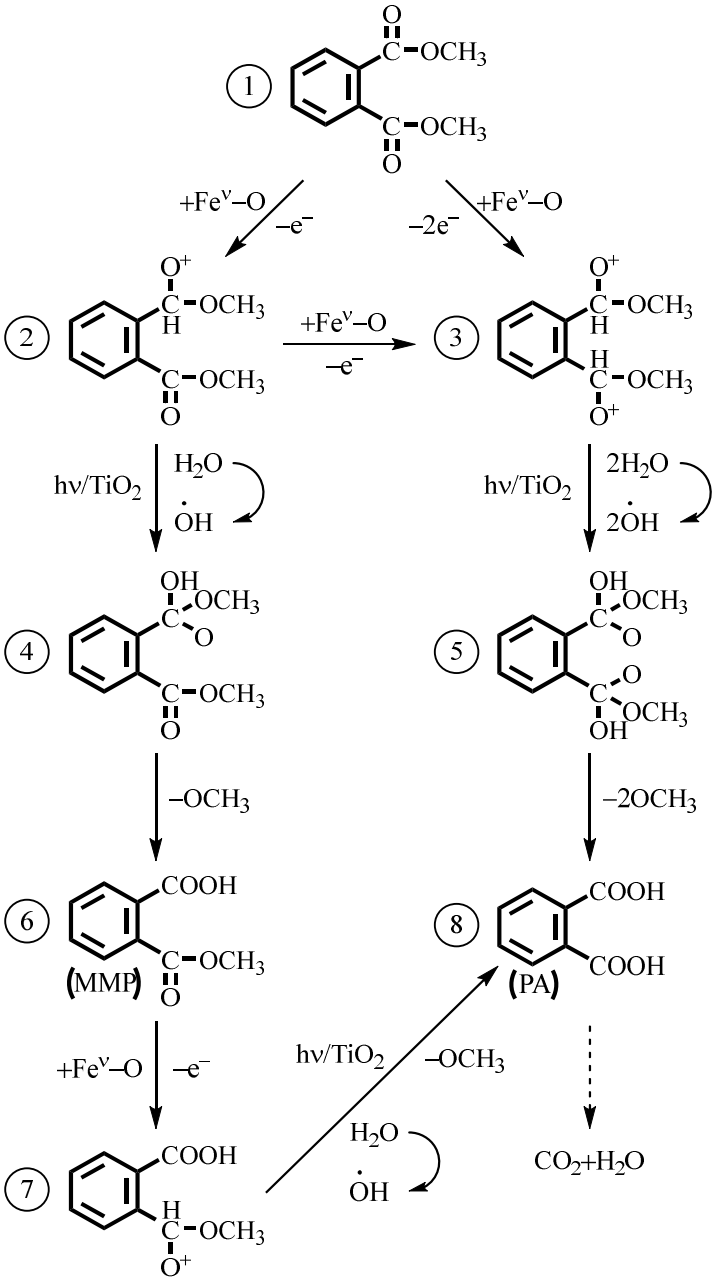

414

415 **Fig. 7** Photocatalytic degradation scheme for DMP by Fe(VI)/TiO_2 under UV-light irradiation.

In the proposed degradation pathway, the major pathway involved a single electron transfer that led to Fe(V) and a radical cationic intermediate resulting in CO_2 extrusion.

Mineralization of DMP in the plastic production wastewater

In order to study the water treatment applications of Fe(VI)/TiO_2/UV system for the mineralization of DMP from complex water matrix, a secondary production wastewater was collected from Changzhou Juli Plastics Co., Ltd in Jiangsu Province, China. The inflow and effluent of secondary wastewater effluents in this plant are 100 m^3 d^{-1} and 96 m^3 d^{-1}, respectively. The characteristics of secondary wastewater effluents were summarized in Table S2. Comparatively, the mineralization efficiencies of DMP in actual wastewater (87.1%) was slightly lower than that in simulated water (95.2%), as presented in Fig. 8(a). This inhibition effect was rationalized by considering that the natural organic matter and some ions (such as CO_3^{2-}) in actual wastewater could compete for Fe(VI) with DMP. Meanwhile, the results of simulated water demonstrated that almost 100% DMP could be effectively photodegraded by Fe(VI)/TiO_2/UV process within 100 min, and the reaction rate constant was as high as 0.271 min^{-1}. The above results illustrated that the Fe(VI)/TiO_2/UV process was a feasible approach for degrading DMP in production wastewater.

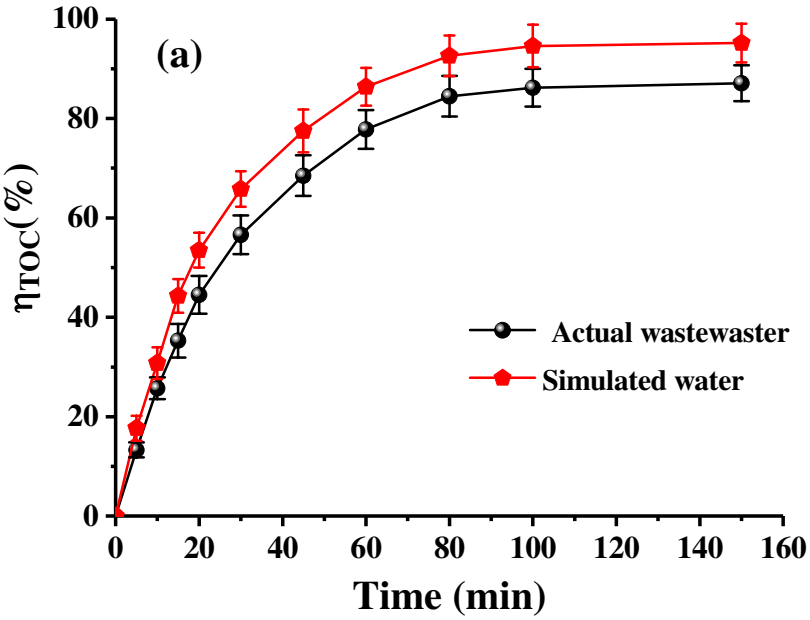
(a)
η_{TOC}(%)
Time (min)
Actual wastewaster
Simulated water
0
20
40
60
80
100
120
140
160

432

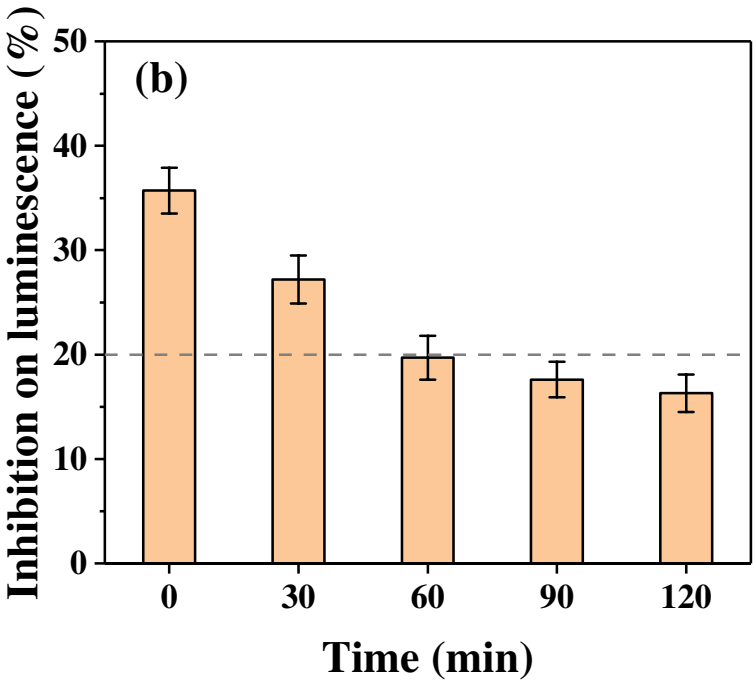
(b)
Inhibition on luminescence (%)
Time (min)
0
10
20
30
40
50
0
30
60
90
120

433

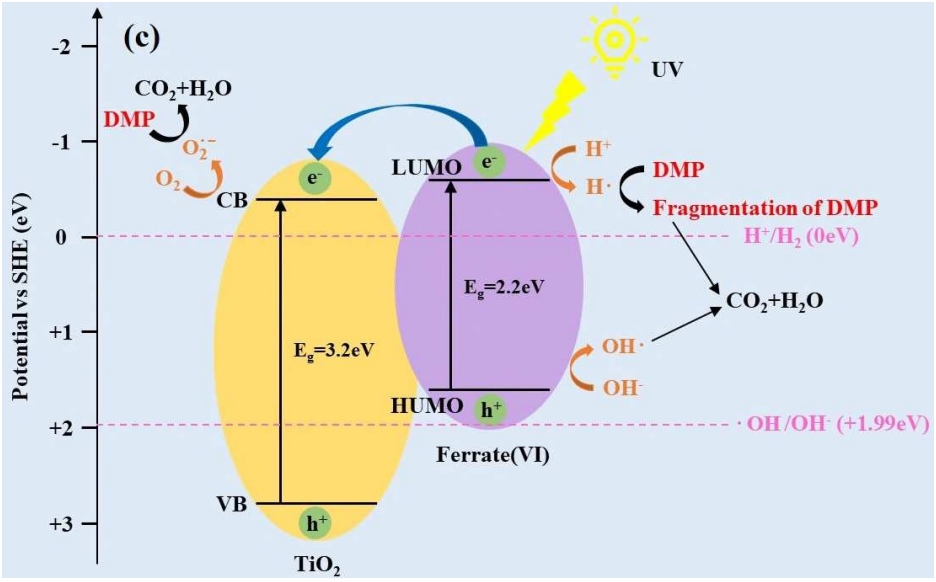

Fig. 8 (a) Mineralization efficiencies (η_{TOC}, %) of DMP in actual and simulated water samples. (b) Dynamic inhibition on luminescence of *Vibrio fischeri* after 15 min of assay time during Fe(VI)/TiO_2/UV treatment of the actual plastic wastewater (Treatment condition: pH 9.0, $[DMP]_0$ = 0.33 mg L^{-1}, $[K_2FeO_4]_0$ = 30.0 mg L^{-1}, $[TiO_2]$ = 50.0 mg L^{-1}, temperature 25.0 ± 1.0°C and treatment time: 120 min). Error bars represent SD from n = 3 replicates. (c) Ultraviolet light photocatalytic pictorial representation for the Fe(VI)/Ti_2O catalyst.

Figure 8(c) demonstrates the ultraviolet light photocatalytic pictorial representation for DMP degradation, using Fe(VI)/TiO_2 as a photocatalyst. First, the conduction band electrons (e_{cb}^-) and valence band holes (h_{vb}^+) are generated when TiO_2 surface absorbs photons (UV radiation) with UV light energy larger than its band gap (Eq.1). Then, the photogenerated electron-hole pairs (excitons) separate apart, the free electrons transfer towards the conduction band and the holes to the valence band at the interface of Fe(VI)/TiO_2, where the photogenerated holes can oxidize DMP molecules (Eq. 13), or react with water and OH^- to form hydroxyl radicals, OH•, the main oxidizing species (Eqs. 11 and 12). The heterogeneous photocatalytic degradation of DMP was illustrated by the following equations.

$$TiO_2 + h\nu \rightarrow h_{vb}^+ + e_{cb}^- \quad \text{(Eq.1)}$$

$$E^\circ = 3.2\ V$$

$$FeO_4^{2-} + 8H^+ + 3e^- \rightarrow Fe^{3+} + 4H_2O \quad \text{(Eq.2)}$$

$E^\circ = 2.2$ V

$H_2O + h_{vb}^+ \rightarrow OH\bullet + H^+$ (Eq.11)

$OH^- + h_{vb}^+ \rightarrow OH\bullet$ (Eq.12)

$DMP + h_{vb}^+ \rightarrow$ oxidation products (Eq.13)

$DMP + OH\bullet \rightarrow$ degradation products (Eq.14)

In order to confirm the effective radicals during photocatalytic process, two chemicals, dimethyl sulphoxide (DMSO, an electron scavenger) and tert-butanol (an OH• scavenger), were used as scavengers for electrons and radicals trapping experiments. As shown in Fig. 8(a), the presence of 1 mmol/L tert-butanol and 1 mmol/L DMSO in the photo-catalytic system show a notable inhibitory effect on the degradation of DMP with Fe(VI)/TiO_2/UV system. Finally, the reusability of the modified TiO_2 was investigated, as shown in Fig. 3(d). The catalyst after one reaction for 120 min was washed with methanol, dried under vacuum, and then reused for the same test. The results indicated that there was almost no obvious reduction of photocatalytic efficiency after nine cycles.

Ecotoxicity evaluation

The acute ecotoxicity of the treated effluent from the reactor was evaluated *via* the change of luminescence intensity of *Vibrio fischeri* after exposure for 15 min (Fig. 8(b)). When the initial concentration of DMP was 0.33 mg/L and treatment time was 120 min, the inhibition changed with time because of the evolution of different byproducts. During the photocatalytic period, the inhibition on luminescence decreased significantly and the samples after treating for 60 min exhibited toxicity below 20%. Thereafter, 16.3% inhibition on the bioluminescence was tested after treating for 120 min. Different from our observation, a significant increment of

475 inhibition (rose to over 40%) during wastewater treatment by Ti/TiO_2 films was discovered,
476 which could be due to the higher concentration employed (Olvera-Vargas et al. 2016). Notably,
477 the inhibition on *Vibrio fischeri* might also ascribe to the residual iron and hydroxyl radical
478 involved in samples therefore the removal of these compounds could further reduce adverse
479 effects on aquatic beings (Tufail et al. 2021). In total, the minor inhibition of 16.3% on the
480 luminescence of *Vibrio fischeri* indicated the Fe(VI)/TiO_2/UV treated effluent would not
481 significantly affect the microorganisms in aquatic environments.

482 **Conclusion**

483 The photocatalytic oxidation of DMP has been investigated by means of UV irradiation
484 over Fe(VI)/TiO_2 catalysts. The major conclusions drawn from this work are summarized as
485 follows:

486 (1) RSM was used to optimize the experimental variables. The 3-D response surface plots
487 indicated that the correlations between pH and K_2FeO_4 dosage, TiO_2 dosage and K_2FeO_4
488 dosage were highly significant. A maximum DMP removal of 95.2 % was achieved under
489 these optimum conditions.

490 (2) The degradation efficiency of DMP in Fe(VI)/TiO_2/UV system was better than that of
491 K_2FeO_4 and TiO_2 alone, indicating that there was a synergistic effect on K_2FeO_4/TiO_2 under
492 UV illumination. Experiments shown that the Fe-O-(organic) complex on the surface of
493 Fe(VI)/TiO_2 could inhibited DMP degradation, and the deactivated TiO_2 catalyst could be
494 reactivated by washed with 1% HCl solution.

495 (3) The intermediates of DMP were identified as MMP and PA by GC-MS. A plausible

degradation pathway was proposed based on the detected intermediates. The free radicals generated by the Fe(VI)/TiO_2/UV system firstly attacked the side chain of DMP, in which MMP as the first metabolite was generated through de-esterification, sequentially followed by the generation of phthalic acid (PA) after further de-esterification of MMP. Eventually, the PA and other low molecular weight organics were mineralized all the way to CO_2 and H_2O.

(4) Combined Fe(VI)/TiO_2 could mineralize 87.1% and 95.2% of DMP from the actual wastewater and simulated water samples under UV illumination. Recycling performance of Fe(VI)/TiO_2/UV system exhibits high activity and stability after nine consecutive-cycles and can be used repeatedly in the decontamination of plastic industrial wastewater.

(5) The ecotoxicity values of wastewater decreased after the Fe(VI)/TiO_2/UV treatment. The treated water samples were non toxic (the decrease in the luminescence of the *Vibrio fischeri* < 20%).

Supplementary data Supplementary data associated with this article can be found online at https://doi.....,

Availability of data and materials All data generated or analyzed during this study are included in this published article (and its supplementary data files).

Authors contribution Ping Wang: funding acquisition, methodology, supervision, validation, writing (review and editing); Liting Zhu and Yunhao Zhang: performed the catalytic tests, analyzed, and interpreted the results of the catalytic activity of the Fe(VI)/TiO_2/UV system; Yi Ding and Sijie Zhou: investigation, data analysis, RSM software; Linbei Xie and Ao Li: formal analysis, validation. The first draft of the manuscript was written by Liting Zhu. All authors read and approved the final manuscript.

Funding This research was financially supported by National Natural Science Foundation of China (grant numbers: 30771696, 31270680) and Jiangsu University Advantages Construction Project Funding Project.

Declarations

Competing interests The authors declare no competing interests.

Ethical approval This article does not contain any studies with human participants or animals performed by any of the authors.

Consent to participate Not applicable.

Consent to publish Not applicable.

References

APHA (2012) Standard Methods for the Examination of Water and Wastewater. 22nd Edition, American Public Health Association, Washington DC.

EL-Mekkawi DM, Abdelwahab NA, Mohamed WAA, Taha NA, Abdel-Mottaleb MS (2020) A Solar photocatalytic treatment of industrial wastewater utilizing recycled polymeric disposals as TiO_2 supports. J Clean Prod 249: 119430.

Graham N, Jiang CC, Li XZ, Jiang JQ, Ma J (2004) The influence of pH on the degradation of phenol and chlorophenols by potassium ferrate. Chemosphere 56 (10): 949–956.

Hu J, Yang Q, Wang JL (2015) Biodegradation of di-n-butyl phthalate in sequencing batch reactor bioaugmented with *Micrococcus* sp. and the bacterial community analysis. Int J Environ Sci Technol 12: 2819–2828.

Jia HZ, Cao Y, Qu GZ, Wang TC, Guo XT, Xia TJ (2018) Dimethyl phthalate contaminated soil remediation by dielectric barrier discharge: performance and residual toxicity. Chem Eng J 351: 1076–1084.

Jing WW, Li DQ, Li J, Li XF, Wu ZH, Liu YL (2018) Photodegradation of dimethyl phthalate (DMP) by UV–TiO_2, in aqueous solution: operational parameters and kinetic analysis. Int J Environ Sci Technol 15: 1–8.

Konstantinou IK, Albanis TA (2004) TiO_2-assisted photocatalytic degradation of azo dyes in aqueous solution: kinetic and mechanistic investigations: A review. Appl Catal B: Environ 49: 1–14.

Lei Y, Zhu CZ, Lu J, Chen R, Xiao J, Peng SC (2018) Photochemical transformation of dimethyl phthalate (DMP) with N(iii)(H_2ONO^+/HONO/NO_2^-) in the atmospheric aqueous environment. Photochem Photobiol Sci 17: 332–341.

Li B, Liu RX, Gao HJ, Tan RJ, Zeng P, Song YH (2016) Spatial distribution and ecological risk

assessment of phthalic acid esters and phenols in surface sediment from urban rivers in Northeast China. Environ Pollut 219: 409–415.
Li C, Li XZ, Graham N (2005) A study of the preparation and reactivity of potassium ferrate. Chemosphere 61: 537–543.
Linsebigler AL, Lu G, Yates JT (1995) Photocatalysis on TiO_2 surfaces: principles, mechanisms, and selected results. Chem Rev 95: 735–758.
Ma Y, Zhang KJ, Li C, Zhang TQ, Gao NY (2015) Oxidation of sulfonamides in aqueous solution by UV-TiO_2-Fe(VI). Biomed Res Int 2015: 942–937.
Maness PC, Smolinski S, Blake DM, Huang Z, Wolfrum EJ, Jacoby WA (1999) Bactericidal activity of photocatalytic TiO_2 reaction: toward an understanding of its killing mechanism. Appl Environ Microbiol 65: 4094–4098.
Martine B, Marie-Jeanne T, Cendrine D, Fabrice A, Marc C (2013) Assessment of adult human exposure to phthalate esters in the urban centre of Paris (France). Bull Environ Contam Toxicol 90: 91–96.
Olvera-Vargas H, Cocerva T, Oturan N, Buisson D, Oturan MA (2016) Bioelectro-Fenton: a sustainable integrated process for removal of organic pollutants from water: application to mineralization of metoprolol. J Hazard Mater 319: 13–23.
Priyanka K, Remya N, Behera M (2019) Comparison of titanium dioxide based catalysts preparation methods in the mineralization and nutrients removal from greywater by solar photocatalysis. J Clean Prod 235: 1-10.
Sarti A, Pozzi E, Chinalia FA, Zaiat M, Foresti E (2006) The performance of an anaerobic sequencing batch biofilm reactor treating domestic sewage colonized by anoxygenic phototrophic bacteria. Chemosphere 62: 1437–1443.
Sharma VK, Burnett CR, Rivera W, Joshi VN (2001) Heterogeneous photocatalytic reduction of ferrate(VI) in UV-irradiated Titania suspensions. Langmuir 17: 4598–4601.
Sharma VK, Graham NJD, Li XZ, Yuan BL (2010) Ferrate(VI) enhanced photocatalytic oxidation of pollutants in aqueous TiO_2 suspensions, Environ Sci Pollut Res 17: 453–461.
Şolpan D, Mehrnia M (2018) Dimethyl phthalate (DMP) degradation in aqueous solution by gamma-irradiation/H_2O_2. J Radioanal Nucl Chem 317: 1–11.
Staples CA, Peterson DR, Parkerton TF, Adams WJ (1997) The environmental fate of phthalate esters: a literature review. Chemosphere 35: 667–749.
Tufail A, Alharbi S, Alrifai J, Ansari A, Price WE, Hai FI (2021) Combining enzymatic membrane bioreactor and ultraviolet photolysis for enhanced removal of trace organic contaminants: Degradation efficiency and by-products formation. Process Saf Environ 145: 110–119.
Turan NB, Erkan HS, Engin GO (2021) Microplastics in wastewater treatment plants: Occurrence, fate and identification. Process Saf Environ 146: 77–84.
Wang W, Wu FY, Huang MJ, Kang Y, Cheung KC, Wong MH (2013) Size fraction effect on phthalate esters accumulation, bioaccessibility and in vitro cytotoxicity of indoor/outdoor dust, and risk assessment of human exposure. J Hazard Mater 261: 753–762.
Wang WX, Fan CQ (2014) Gas/solid particulate phthalic esters (PAEs) in Masson pine (*Pinus massoniana* L.) needles and rhizosphere surface soils. J Hazard Mater 276: 149– 156.
Wang WX, Xu XB, Fan CQ (2015) Health hazard assessment of occupationally di-(2-ethylhexyl)-phthalate-exposed workers in China. Chemosphere 120: 37–44.
Wang WX, Zhang YL, Wang SL, Fan CQ, Xu H (2012) Distributions of phthalic esters carried

by total suspended particulates in Nanjing, China. Environ Monit Assess 184: 6789–6798.
Winkelmann K, Sharma VK, Lin YA, Shreve KA, Winkelmann C, Hoisington LJ, Yngard RA, Wong CC, Chu W (2008) Reduction of ferrate(VI) and oxidation of cyanate in a Fe(VI)–TiO_2 –UV–NCO- system. Chemosphere 72: 1694–1699.
Wong CC, Chu W (2003) The hydrogen peroxide-assisted photocatalytic degradation of alachlor in TiO_2 suspensions. Environ Sci Technol 37: 2310–2316.
Wood RH (1958) The second ionization constant of hydrogen selenide. J Am Chem Soc 80: 1559–1562.
Yuan BL, Qu JH, Fu ML (2002) Removal of cyanobacterial microcystin-LR by ferrate oxidation-coagulation, Toxicon 40: 1129–1134.
Zhang LL, Liu JL, Liu HY, Wan GS, Zhang SW (2015) The occurrence and ecological risk assessment of phthalate esters (PAEs) in urban aquatic environments of China. Ecotoxicology 24: 1–18.
Zhou LJ, Gu W, Liu JN, Shi LL, Xu YH (2017) Fate of eleven phthalic acid esters in aerobic sewage treatment system. Environ Sci 38: 1972–1981.

Supplementary Files

This is a list of supplementary files associated with this preprint. Click to download.

- 0407ResearchData.docx
- 20200417Supplementary.doc